

# Theory of dynamical phase transitions in collective quantum systems

Ángel L. Corps<sup>1,2,\*</sup> and Armando Relaño<sup>2,3,†</sup>

<sup>1</sup>*Instituto de Estructura de la Materia, IEM-CSIC, Serrano 123, E-28006 Madrid, Spain*

<sup>2</sup>*Grupo Interdisciplinar de Sistemas Complejos (GISC),*

*Universidad Complutense de Madrid, Av. Complutense s/n, E-28040 Madrid, Spain*

<sup>3</sup>*Departamento de Estructura de la Materia, Física Térmica y Electrónica,*

*Universidad Complutense de Madrid, Av. Complutense s/n, E-28040 Madrid, Spain*

(Dated: May 10, 2022)

We present a theory for the two kinds of dynamical quantum phase transitions, sometimes termed DPT-I and DPT-II, in collective many-body systems. Both are triggered by excited-state quantum phase transitions. For quenches below the critical energy, the existence of an additional conserved charge, identifying the corresponding phase, allows for a non-zero value of the dynamical order parameter characterizing DPTs-I, and precludes the mechanism giving rise to non-analyticities in the return probability, trademark of DPTs-II. We propose a statistical ensemble describing the long-time averages of order parameters in DPTs-I, and provide a theoretical proof for the absence of true DPT-II critical times in the thermodynamic limit in the phase with this additional conserved charge. Our results are numerically illustrated in the fully-connected transverse-field Ising model, which exhibits both kinds of dynamical phase transitions.

**Introduction.**– Recent advances in experimental techniques with cold atoms and trapped ions [1–5] have stimulated the research about some fundamental concepts. Dynamical quantum phase transitions (DPTs) are one of them. The term refers to two distinct phenomena. The first one, DPT-I, occurs when the dynamics of observables qualitatively changes at a critical value of a control parameter [6–11]. DPTs-I are characterized by a dynamical order parameter, given by the long-time average of an observable which changes from a nonzero value to zero at the critical value of the control parameter (for a recent review, see [12]). The second one, DPT-II, happens when the dynamics becomes non-analytic at particular critical times [13–19]; hence, it is a purely non-equilibrium phenomenon which cannot be described by a dynamical order parameter. Both kinds of DPTs may appear in the same models, for example the long-range or fully connected transverse-field Ising model [20, 21], or the Rabi model [22]. However, although connections between them have been found [20, 21, 23–27], a common mechanism for their appearance is missing [28].

In this Letter, we present a theory showing that these two kinds of DPTs share a common origin in *collective* quantum systems. This link is driven by excited-state quantum phase transitions (ESQPTs) [29], which entail abrupt changes in the way a closed system thermalizes after a non-equilibrium process [30–35]. The key point lies on our recent proposal that the critical energy of an ESQPT splits the spectrum into two different phases: one in which there exists a constant of motion,  $\hat{C}$ , acting like a partial dynamical symmetry, and another in which this operator is no longer constant [36]. Our results show that, in collective many-body systems with a discrete  $\mathbb{Z}_2$  symmetry, (i) the dynamical order parameter characterizing DPTs-I can be different from zero if and only if  $\hat{C}$  is a constant of motion, and (ii) the constancy of  $\hat{C}$  precludes the mechanism responsible of DPT-II in systems with a discrete  $\mathbb{Z}_2$  symmetry [14]. This means that both kinds of DPTs are triggered by the behavior of  $\hat{C}$  and therefore by the ESQPT. We illustrate these findings by numerical experiments in the

fully connected transverse-field Ising model [20, 21].

**Setup.**– Let us consider a collective Hamiltonian,  $\hat{H}(\lambda)$ , depending on a control parameter,  $\lambda$ , with the following features. First, it has a discrete  $\mathbb{Z}_2$  symmetry, represented by a discrete operator  $\hat{\Pi}$ , which we call parity, fulfilling  $[\hat{H}(\lambda), \hat{\Pi}] = 0, \forall \lambda$ . Second, the control parameter has a critical value,  $\lambda_c$ , at which a quantum phase transition (QPT) [37] occurs. If  $\lambda > \lambda_c$ , the ground state is two-fold degenerate in the thermodynamic limit (TL), and gives rise to a broken-symmetry phase. Contrarily, if  $\lambda < \lambda_c$ , the ground state is unique with a well-defined parity. And third, the broken-symmetry phase at  $\lambda > \lambda_c$  extends up to a certain critical energy,  $E_c$ , at which an ESQPT takes place; below this energy, the spectrum is composed by parity doublets exactly degenerate in the TL [29, 36]. As typical examples, we quote the Lipkin-Meshkov-Glick (LMG) model [38–46], the Dicke and Rabi models [47–54], spinor Bose-Einstein condensates [55], the coupled top [56] and the two-site Bose-Hubbard model [57].

In a recent paper [36], we showed that this setup has two different excited-state phases for  $\lambda > \lambda_c$ . Below the critical energy of the ESQPT, signaled by a non-analyticity in the density of states, there exists an additional conserved charge,  $\hat{C}$ , with just two eigenvalues,  $\text{Spec}(\hat{C}) = \{\pm 1\}$ , which acts like a partial  $\mathbb{Z}_2$  symmetry. Its origin lays in the semiclassical limit of the Hamiltonian, whose phase space consists of two disjoint regions for  $E < E_c$ . The operator  $\hat{C}$  labels to which of them a given eigenfunction is attached to. An important feature is that  $\hat{C}$  is *not* commuting with  $\hat{\Pi}$ . For  $E > E_c$  the semiclassical phase space becomes connected, and  $\hat{C}$  is no longer a conserved charge [36, 58, 59]. In the rest of this Letter, we derive a theory, and test it numerically, showing how the behavior of  $\hat{C}$  triggers both kinds of DPTs.

**Theory for DPTs-I.**– If a closed quantum system reaches an equilibrium state, this state is equal to the infinite-time average of the real time-evolved wavefunction [60]. This means that long-time averages, giving rise to dynamical order parameters for DPTs-I, can be described by means of equilibrium ensem-

bles, regardless of whether they are real equilibrium states or just effective states around which the system oscillates. Hence, our first aim is to build an equilibrium ensemble, depending on all the relevant constants of motion, for our setup. Above  $E_c$ , such ensemble must depend only on energy and parity; it must be diagonal in a parity eigenbasis. Below  $E_c$ , it must depend also on  $\hat{C}$ ; as  $[\hat{\Pi}, \hat{C}] \neq 0$ , it must be non-diagonal in the same basis, and therefore it must store information about quantum coherences between parity sectors. As these coherences are complex-valued, a real operator like  $\hat{C}$  cannot account for all their possible values. Therefore, we propose a second operator which is also constant below the critical energy,

$$\hat{\mathcal{K}} \equiv \frac{i}{2} [\hat{C}, \hat{\Pi}]. \quad (1)$$

It is straightforward to show that  $\hat{\mathcal{K}}$  commutes with the energy projectors below the critical energy if  $\hat{C}$  does too [61]. Hence, our generic system is characterized by a set of three non-commuting charges,  $\{\hat{\Pi}, \hat{C}, \hat{\mathcal{K}}\}$  for  $E < E_c$ , whereas only  $\hat{\Pi}$  is a constant of motion above  $E_c$ . At first sight, this seems to imply that we need two equilibrium ensembles to describe our setup, and that the transient region is somehow ill-defined. However, we can fix this problem defining two new operators to be used instead of  $\hat{C}$  and  $\hat{\mathcal{K}}$ ,

$$\tilde{C} = \mathbb{I}_{E < E_c} \hat{C} \mathbb{I}_{E < E_c}, \quad (2)$$

$$\tilde{K} = \mathbb{I}_{E < E_c} \hat{\mathcal{K}} \mathbb{I}_{E < E_c}. \quad (3)$$

where  $\mathbb{I}_{E < E_c} \equiv \sum_n \theta_n \hat{P}_n$ ,  $\hat{P}_n$  is the projector onto the eigenspace with energy  $E_n$ , and  $\theta_n = 1$  if  $E_n < E_c$  and  $\theta_n = 0$  if  $E_n > E_c$ .  $\tilde{C}$  and  $\tilde{K}$  are equal to  $\hat{C}$  and  $\hat{\mathcal{K}}$  below the critical energy of the ESQPT, but identically zero above it. This means that  $\tilde{C}$  and  $\tilde{K}$  commute with the Hamiltonian in the TL, and therefore we can build an unique equilibrium ensemble from them.

Next, we use these operators to build a statistical ensemble for our setup. The simplest choice is [61]

$$\rho_{\text{GME}}(E, p, c, k) = \rho_{\text{ME}}(E) \left( \mathbb{I} + p \hat{\Pi} + c \tilde{C} + k \tilde{K} \right), \quad (4)$$

where  $\rho_{\text{ME}}(E)$  denotes the standard microcanonical ensemble [62], in which all parity doublets,  $|E_{n,+}\rangle$  and  $|E_{n,-}\rangle$ , within a small energy window around the average energy value,  $\langle E \rangle = \text{Tr}[\hat{\rho}_{\text{GME}} \hat{H}]$ , are equally populated, and  $\text{Tr} \rho_{\text{GME}}(E) = 1$ . We call  $\rho_{\text{GME}}(E, p, c, k)$  *generalized microcanonical ensemble* (GME). Besides the average energy, it depends on three free parameters,  $p, c, k \in \mathbb{R}$ ,  $p^2 + c^2 + k^2 \leq 1$ , which are fixed by requiring that  $\text{Tr}[\rho_{\text{GME}} \hat{\Pi}] = \langle \hat{\Pi} \rangle$ ,  $\text{Tr}[\rho_{\text{GME}} \tilde{C}] = \langle \tilde{C} \rangle$ , and  $\text{Tr}[\rho_{\text{GME}} \tilde{K}] = \langle \tilde{K} \rangle$ . It is an example of an equilibrium ensemble depending on non-commuting charges [63–65].

This ensemble has the following properties:

(i) It accounts for the quantum coherences between parity sectors if and only if  $E < E_c$ .  $\rho_{\text{GME}}(E, p, c, k)$  has non-diagonal elements in the parity eigenbasis if  $c \neq 0$  and/or  $k \neq 0$ . As a consequence, the expectation value of parity-changing observables, like  $\text{Tr}[\rho_{\text{GME}}(E, p, c, k) \hat{J}_x]$ , may be different from zero only in this region.

(ii) It becomes diagonal when all populated states are above  $E_c$ . Hence, if  $E > E_c$ ,  $\text{Tr}[\rho_{\text{GME}}(E, p, c, k) \hat{J}_x] = 0$  for any initial condition.

These two properties imply that *a DPT-I happens when a quench crosses the critical energy of the ESQPT*. If the initial state fulfills  $E < E_c$  and the quench leads the system to a region where all populated states have energy above  $E_c$ , then all information about quantum coherences between parity sectors is lost.

*Numerical results: DPTs-I.* To test our theory, we choose the transverse-field Ising model, which coincides with a version of the LMG Hamiltonian [38],

$$\hat{H}(\lambda) = -\frac{\lambda}{4N} \sum_{i,j=1}^N \hat{\sigma}_i^x \hat{\sigma}_j^x + \frac{h}{2} \sum_{i=1}^N \hat{\sigma}_i^z = -\frac{\lambda}{N} \hat{J}_x^2 + h \hat{J}_z. \quad (5)$$

Here,  $\hat{\sigma}_{x,y,z}$  are the Pauli matrices, and  $\hat{\mathbf{J}} = (\hat{J}_x, \hat{J}_y, \hat{J}_z)$  is the collective angular momentum for the  $N$  1/2-spins that form the system, which is an exact conserved quantity,  $[\hat{H}(\lambda), \hat{\mathbf{J}}^2] = 0$ . Hence we can separate the Hamiltonian matrix in symmetry sectors according to its eigenvalues,  $j(j+1)$ ; we focus on the maximally symmetric sector,  $j = N/2$ . In what follows, we fix  $h = 1$ , and consider  $\lambda$  as the control parameter. This choice is equivalent to the typical procedure in which  $\lambda$  is kept fixed and  $h$  is taken as the control parameter [10, 11, 15], and allows us to identify the critical points in simpler terms. In experiments such as [11], the magnetic field is on the scale  $h \sim \text{MHz}$ ; this implies that in our numerical results,  $t \sim \mu\text{s}$ .

This model has a QPT at  $\lambda_c = h$  [61, 66]. For  $\lambda > \lambda_c$ , it also exhibits an ESQPT exactly at  $\epsilon_c \equiv E_c/j = -h$  in the TL, signaled by a logarithmic singularity in its level density [39–45, 61]. For  $\lambda > \lambda_c$  and  $E < E_c$ , the LMG model displays a broken-symmetry phase where the eigenstates of different parity,  $\hat{\Pi} \equiv e^{i\pi(j+\hat{J}_z)}$ , are degenerate,  $E_{n,+} = E_{n,-}$  where  $\hat{\Pi}|E_{n,\pm}\rangle = \pm|E_{n,\pm}\rangle$ . However, if  $\lambda < \lambda_c$ , or  $\lambda > \lambda_c$  and  $E > E_c$ , this degeneracy is lifted,  $E_{n,+} \neq E_{n,-}$  and the  $\mathbb{Z}_2$  symmetry is restored. Below  $E_c$ ,  $\hat{C} = \text{sign}(\hat{J}_x)$  is a conserved charge, and  $\hat{\mathcal{K}}$  can be obtained from Eq. (1) (see [61] for a detailed semiclassical analysis).

DPTs-I can be identified in this model via the dynamics of  $\hat{J}_x$  [10, 11, 15], i.e., by starting from a broken-symmetry ground state, quenching the system and studying the time-evolution of  $\hat{J}_x$ . Here, we follow the same strategy. We start from a superposition of the two degenerate ground states,  $E_{0,\pm} < E_c$ , at an initial value of the control parameter,  $\lambda_i > \lambda_c$ ,

$$|\Psi_0(\lambda_i)\rangle = \sqrt{\alpha}|E_{0,+}(\lambda_i)\rangle + e^{i\phi}\sqrt{1-\alpha}|E_{0,-}(\lambda_i)\rangle, \quad (6)$$

where  $\alpha \in [0, 1]$  and  $\phi \in [0, 2\pi]$ . Recent experimental realizations [10, 11, 15] follow the same protocol with  $\alpha = 1/2$  and  $\phi = 0$ . In this state, we have  $\langle \hat{\Pi} \rangle = 2\alpha - 1$ ,  $\langle \hat{C} \rangle = 2\sqrt{\alpha(1-\alpha)} \cos \phi$ , and  $\langle \hat{\mathcal{K}} \rangle = 2\sqrt{\alpha(1-\alpha)} \sin \phi$ . Then, we quench the system to  $\lambda_f$ , and allow a unitary time evolution,  $|\Psi_t(\lambda_f)\rangle = e^{-i\hat{H}(\lambda_f)t}|\Psi_0(\lambda_i)\rangle$ .

In Fig. 1 we focus on three different quenches with  $\lambda_f = 1.75$ ,  $j = 6400$ , and  $\alpha = 3/4$  and  $\phi = \pi/6$ . Fig. 1(a-c)

shows the eigenstate populations after the quench,  $P(E) = \sum_n \sum_{k=\pm} |\langle E_{n,k}(\lambda_f) | \Psi_0(\lambda_i) \rangle|^2 \delta(E - E_{n,k})$ , for  $\lambda_i = 2.5$ ,  $\lambda_i = 7$ , and  $\lambda_i = 27.5$ , respectively. The huge fluctuations in  $P(E)$  are due to the occupation of positive-parity eigenstates being three times larger than the occupation of negative-parity eigenstates.

The dynamical consequences of these quenches are shown in Fig. 1(d-g); we represent the time evolution  $\langle \hat{J}_z(t) \rangle = \langle \Psi_t(\lambda_f) | \hat{J}_z | \Psi_t(\lambda_f) \rangle$ ,  $\langle \hat{J}_x(t) \rangle$ ,  $\langle \hat{C}(t) \rangle$ , and  $\langle \hat{K}(t) \rangle$ , with the corresponding GME theoretical predictions. We observe that the GME provides a perfect description of long-time averages in all cases. For  $\langle \hat{J}_z(t) \rangle$ , shown in Fig. 1(d), we see no traces of DPTs. So, let us first focus on the usual dynamical order parameter,  $\langle \hat{J}_x(t) \rangle$ , shown in Fig. 1(e). For short times, it oscillates following the semiclassical expectation [61], and then relaxes to a pseudo-equilibrium state [12]. Most importantly, its long-time average,  $\langle \hat{J}_x \rangle \equiv \lim_{\tau \rightarrow \infty} (1/\tau) \int_0^\tau dt \langle \hat{J}_x(t) \rangle$ , is only zero above  $E_c$  (blue). Below this energy,  $\langle \hat{J}_x(t) \rangle$  oscillates and relaxes towards a value clearly different from zero (red), and this also happens when the quench leads the system to the critical energy of the ESQPT (magenta). These observations are easily explained by the GME. As shown in Fig. 1(f-g),  $\langle \hat{C} \rangle$  and  $\langle \hat{K} \rangle$  are also different from zero for the two first quenches, meaning that  $c \neq 0$  and  $k \neq 0$  in both cases. Note also that these two observables are constant for  $E < E_c$ , as expected. At the critical quench, states both below and above  $E_c$  are populated. The former makes it possible to find symmetry-breaking long-time averages with  $c \neq 0$  and  $k \neq 0$ , and the latter implies that  $\hat{C}$  and  $\hat{K}$  are no longer constant. Finally, we have that  $\langle \hat{C} \rangle = \langle \hat{K} \rangle = \langle \hat{J}_x \rangle = 0$  for the last quench, because the parity symmetry is restored in this case. Therefore, these results are fully compatible with our theory.

In Fig. 2 we display the long-time averages of the same observables together with the GME prediction for different quenches. In Fig. 2(a), we observe an abrupt minimum of  $\langle \hat{J}_z \rangle$  at  $E_c$ . But the critical behavior is best observed in  $\langle \hat{J}_x \rangle$ ,  $\langle \hat{C} \rangle$  and  $\langle \hat{K} \rangle$ : these are different from zero only below the critical energy. In the insets of Fig. 2(b-d) we show how the largest energy,  $E_c^*(\gamma)$ , for which  $\langle \hat{J}_x \rangle$ ,  $\langle \hat{C} \rangle$  and  $\langle \hat{K} \rangle$  remain larger than a given bound,  $\gamma$  (see caption of Fig. 2 for details), scales as a function of the system size. This scaling is fully compatible with these long-time averages becoming zero exactly at  $E_c$  in the TL, as predicted by our theory. Furthermore, the GME provides a perfect description of these equilibrium values.

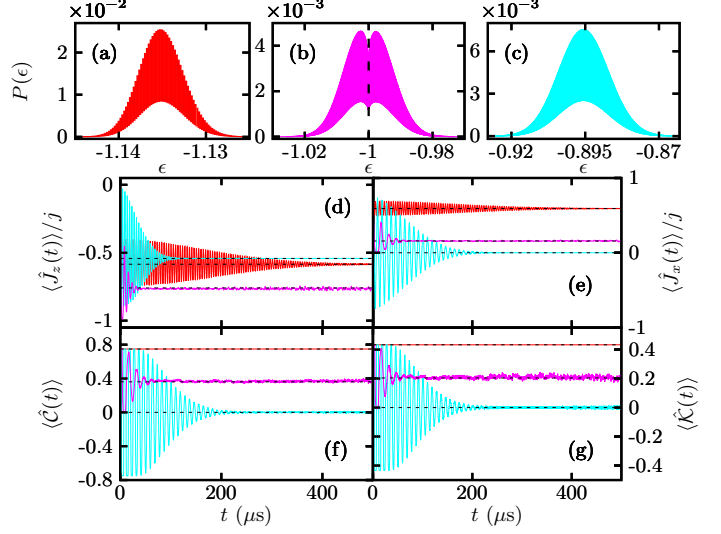


FIG. 1. (a-c) Probability of populated states after a quench  $\lambda_i \rightarrow \lambda_f = 1.75$ . The values of the initial control parameter and the quenched state energy are (a)  $\lambda_i = 2.5$ ,  $E(\lambda_f) = -1.135$  (b)  $\lambda_i = 7$ ,  $E(\lambda_f) = -1$ , and (c)  $\lambda_i = 27.5$ ,  $E(\lambda_f) = -0.89567$ . The black dashed line in (b) represents the ESQPT critical energy. (d-g) Time evolution of physical observables after the quench. Color lines in (d-g) follow the same code as in (a-c). Black dashed lines show the GME predictions, whose energy window is equal to twice the standard deviation of  $P(E)$ . System size is  $j = 6400$ ; the initial state has  $\alpha = 3/4$ ,  $\phi = \pi/6$ .

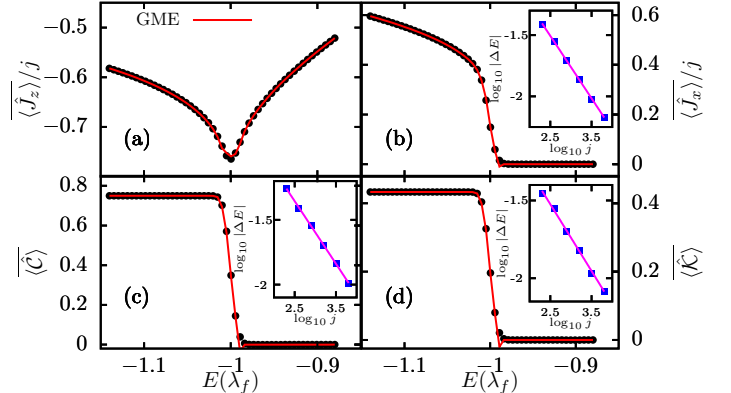


FIG. 2. (a-d) Long-time average of physical observables after a quench  $\lambda_i \rightarrow \lambda_f = 1.75$  as a function of the final energy  $E(\lambda_f)$ . System size is  $j = 6400$ ; the initial state has  $\alpha = 3/4$ ,  $\phi = \pi/6$ . Black points represent the exact averages while red lines show the GME prediction. Insets in (b-d) show the scaling of  $\Delta E = E_c^*(\gamma) - E_c^\infty$  with system size ( $\gamma = 1/20$ ),  $|\Delta E| \sim j^{-a}$ ,  $a > 0$ .

*Theory for DPTs-II.*— In principle, this kind of DPTs has a completely different origin. We again consider a quantum quench  $\lambda_i \rightarrow \lambda_f$  where the initial state  $|\Psi_0(\lambda_i)\rangle$  is the broken-symmetry ground-state at  $\lambda_i > \lambda_c$ ,  $E < E_c$ . In systems with a discrete  $\mathbb{Z}_2$  symmetry, DPTs-II are signaled by non-analytic points in  $P(0, t) \equiv \mathcal{L}_+(t) + \mathcal{L}_-(t)$ , where

$\mathcal{L}_\pm = |\langle E_{0,\pm}(\lambda_i) | \Psi_t(\lambda_f) \rangle|^2$  are the return probabilities to the positive-parity and negative-parity projections of the initial state [14] after the quench. These non-analytic points are usually identified through the rate  $r_N(t) = -\ln P(0, t)/N$ , which can be understood as a dynamical version of the Helmholtz free energy per particle [13]. In general, it is expected that  $\mathcal{L}_\pm = \exp[-N\Omega_\pm(t)]$  [13], where  $\Omega_\pm(t)$  is an intensive ana-

lytical function (see [61] for a detailed discussion). Hence, in the TL the term with the smallest value of  $\Omega_{\pm}$  dominates, and therefore, non-analyticities appear at any crossing point at which  $\Omega_+(t) = \Omega_-(t)$  [14]. As in standard phase transitions,  $r_N(t)$  remains analytic for finite values of  $N$ , and only becomes singular in the TL.

We start with an initial state given by Eq. (6) at  $\lambda_i$ , quenched to  $\lambda_f$ . We then have

$$\mathcal{L}_+(t) = \alpha f_+(t), \quad \mathcal{L}_-(t) = (1 - \alpha) f_-(t), \quad (7)$$

with  $f_{\pm}(t) = |\sum_n |c_{n,\pm}|^2 e^{-iE_{n,\pm}(\lambda_f)t}|^2$ , and the expansion of initial eigenstates  $|E_{0,\pm}(\lambda_i)\rangle = \sum_n c_{n,\pm} |E_{n,\pm}(\lambda_f)\rangle$  allowed by parity conservation. The key point of our theory is the following:

**Result:** If  $E < E_c$ , then  $f_+(t) = f_-(t), \forall t$ .

To prove this, we first recall that  $E_{n,+}(\lambda_f) = E_{n,-}(\lambda_f)$  if  $E_{n,\pm} < E_c$  in the TL [36], meaning that the oscillatory parts in  $f_{\pm}(t)$  coincide. We then focus on  $c_{n,+} = \langle E_{n,+}(\lambda_f) | E_{0,+}(\lambda_i) \rangle$ . As  $\hat{C} |E_{n,\pm}\rangle = \alpha |E_{n,\mp}\rangle$  in the TL whenever  $E_{n,\pm} < E_c$  (with  $\alpha$  an arbitrary sign that can be fixed to +1 [36]), we get

$$\begin{aligned} |c_{n,+}| &= |\langle E_{n,+}(\lambda_f) | E_{0,+}(\lambda_i) \rangle| = \\ &= |\langle E_{n,-}(\lambda_f) | \hat{C}^\dagger \hat{C} | E_{0,-}(\lambda_i) \rangle| = \\ &= |\langle E_{n,-}(\lambda_f) | E_{0,-}(\lambda_i) \rangle| = |c_{n,-}|, \end{aligned} \quad (8)$$

for any eigenspace below the critical energy, where the unitarity of  $\hat{C}$  has been used,  $\hat{C}^\dagger \hat{C} = 1$  [36]. Therefore,  $f_+(t) = f_-(t)$  in the TL, if all the populated states are below the critical energy.

**Consequence:** the constancy of  $\hat{C}$  if  $E < E_c$  implies  $\Omega_+(t)$  and  $\Omega_-(t)$  cannot cross. Therefore *DPTs-II are forbidden for quenches below the critical energy and can only happen if the quench leads the system to  $E > E_c$* .

The result follows from simple algebraic manipulations of Eq. (7) [61].

**Numerical results: DPTs-II.** - We test this result in Fig. 3. We display  $r_N(t)$  for two quenches, one below the critical energy, shown Fig. 3(a), and another above the critical energy, shown Fig. 3(b), both for an initial state Eq. (6) with  $\alpha = 1/2$  and  $\phi = 0$ . The corresponding eigenstate populations are shown in Fig. 3(c-d), respectively. A first glimpse suggests that there are non-analytical points in the two cases, the first ones related to an anomalous dynamical phase [16, 17]. To delve into this preliminary conclusion, we display  $dr_N(t)/dt$  in Fig. 3(e-f). The finite-size scaling in Fig. 3(e), corresponding to the inset of Fig. 3(a), does *not* suggest a true non-analyticity in the TL: the irregularities in  $dr_N(t)/dt$  are more or less the same for all system sizes. Contrarily, Fig. 3(f) shows that  $dr_N(t)/dt$  approaches a discontinuity as  $N$  grows for the kink shown in the inset of Fig. 3(b). Furthermore, all the finite-size curves cross at the finite-size precursor of the critical time,  $t_c \approx 2.68$ . This behavior is reminiscent of first-order phase transitions.

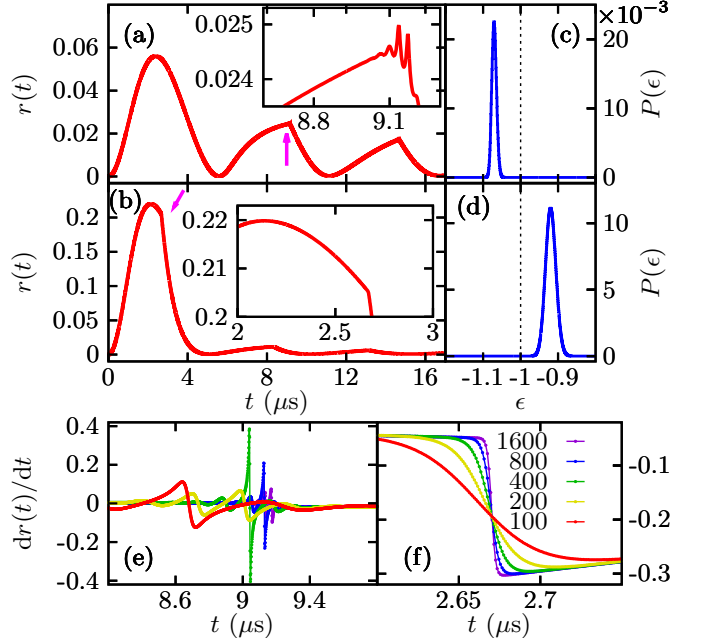


FIG. 3. (a-b)  $r_N(t)$  for a quench from (a)  $\lambda_i = 2.535$  to  $\lambda_f = 1.6$ , and  $j = 1600$ , and (b) quench from  $\lambda_i = 7.437$  to  $\lambda_f = 1.6$ , and  $j = 1600$ ; (c-d) energy distributions for the quenches in (a-b), respectively; (e-f) finite-size scaling of  $dr_N(t)/dt$  around the kinks shown by magenta arrows in (a-b), respectively, for several  $j$  [legend in (f)]. The initial state has  $\alpha = 1/2$  and  $\phi = 0$ .

From our theory, we can interpret these results in the following way. Below the critical energy,  $E < E_c$ ,  $\hat{C}$  is a conserved charge. Therefore, the behavior shown in the inset of Fig. 3(a) cannot be caused by the crossing of  $\Omega_+(t)$  and  $\Omega_-(t)$ , and hence its origin remains unclear [61]. It is worth remarking that this behavior in the TL is also unclear. However, above the critical energy,  $E > E_c$ ,  $\hat{C}$  is no longer a conserved charge, and  $\Omega_+(t)$  and  $\Omega_-(t)$  can cross. Thus,  $r_N(t)$  is expected to become non-analytical at the corresponding crossing times in the TL, as depicted in Fig. 3(f).

**Conclusions.** - In this Letter we have put forward a theory of dynamical phase transitions in collective systems which undergo an ESQPT. In the TL, we propose a dynamical phase diagram composed by two different phases, separated by the critical energy of the ESQPT. Below this critical energy, a set of three non-commuting conserved charges are necessary to describe long-time averages, dynamical order parameters can be different from zero, and the main mechanism for non-analyticities in the return probability is forbidden. Above the ESQPT critical energy, the only conserved charge is parity, representing the  $\mathbb{Z}_2$  symmetry of the system, dynamical order parameters cannot be different from zero, and non-analyticities in the return probability are allowed. Our results are illustrated in the fully connected transverse-field Ising model.

We gratefully acknowledge discussions with P. Pérez-Fernández and J. Dukelsky. This work has been supported by the Spanish grant PGC-2018-094180-B-I00 funded by Minis-

terio de Ciencia e Innovación/Agencia Estatal de Investigación MCIN/AEI/10.13039/501100011033 and FEDER "A Way of Making Europe". A. L. C. acknowledges financial support from 'la Caixa' Foundation (ID 100010434) through the fellowship LCF/BQ/DR21/11880024.

\* [corps.angel.1@gmail.com](mailto:corps.angel.1@gmail.com)

† [armando.relano@fis.ucm.es](mailto:armando.relano@fis.ucm.es)

[1] M. Gring, M. Kuhnert, T. Langen, T. Kitagawa, B. Rauer, M. Schreitl, I. Mazets, D. Adu Smith, E. Demler, and J. Schmiedmayer, *Relaxation and Prethermalization in an Isolated Quantum System*, *Science* **337**, 1318 (2012).

[2] S. Hofferberth, I. Lesanovsky, B. Fischer, T. Schumm, and J. Schmiedmayer, *Non-equilibrium coherence dynamics in a one-dimensional Bose gases*, *Nature* **449**, 324 (2007).

[3] S. Hild, T. Fukuhara, P. Schauß, J. Zeiher, M. Knap, E. Demler, I. Bloch, and C. Gross, *Far-from-equilibrium spin transport in Heisenberg quantum magnets*, *Phys. Rev. Lett.* **113**, 147205 (2014).

[4] E. A. Yuzbashyan, O. Tsypliyatnev, and B. L. Altshuler, *Relaxation and persistent oscillations of the order parameter in fermionic condensates*, *Phys. Rev. Lett.* **96**, 097005 (2006).

[5] K. Baumann, C. Guerlin, F. Brennecke, and T. Esslinger, *Dicke quantum phase transition with a superfluid gas in an optical cavity*, *Nature* **464**, 1301 (2010).

[6] M. Eckstein and M. Kollar, *Nonthermal Steady States after an Interaction Quench in the Falicov-Kimball Model*, *Phys. Rev. Lett.* **100**, 120404 (2008).

[7] M. Moeckel and S. Kehrein, *Interaction Quench in the Hubbard Model*, *Phys. Rev. Lett.* **100**, 175702 (2008).

[8] M. Eckstein, M. Kollar, and P. Werner, *Thermalization after an Interaction Quench in the Hubbard Model*, *Phys. Rev. Lett.* **103**, 056403 (2009).

[9] B. Sciolla and G. Biroli, *Dynamical transitions and quantum quenches in mean-field models*, *J. Stat. Mech.* (2011) P11003.

[10] J. Zhang, G. Pagano, P. W. Hess, A. Kyprianidis, P. Becker, H. Kaplan, A. V. Gorshkov, Z.-X. Gong, and C. Monroe, *Observation of a many-body dynamical phase transition with a 53-qubit quantum simulator*, *Nature* **551**, 601 (2017).

[11] J. A. Muniz, D. Barberena, R. J. Lewis-Swan, D. J. Young, J. R. K. Cline, A. M. Rey, and J. K. Thompson, *Exploring dynamical phase transitions with cold atoms in an optical cavity*, *Nature* **580**, 602 (2020).

[12] J. Marino, M. Eckstein, M. S. Foster, and A. M. Rey, *Dynamical phase transitions in the collisionless pre-thermal states of isolated quantum systems: theory and experiments*, arXiv:2201.09894 (2022).

[13] M. Heyl, A. Polkovnikov, and S. Kehrein, *Dynamical Quantum Phase Transitions in the Transverse-Field Ising Model*, *Phys. Rev. Lett.* **110**, 135704 (2013).

[14] M. Heyl, *Dynamical Quantum Phase Transitions in Systems with Broken-Symmetry Phases*, *Phys. Rev. Lett.* **113**, 205701 (2014).

[15] P. Jurcevic, H. Shen, P. Hauke, C. Maier, T. Brydges, C. Hempel, B. P. Lanyon, M. Heyl, R. Blatt, and C. F. Roos, *Direct Observation of Dynamical Quantum Phase Transitions in an Interacting Many-Body System*, *Phys. Rev. Lett.* **119**, 080501 (2017).

[16] I. Homrighausen, N. O. Abeling, V. Zauner-Stauber, and J. C. Halimeh, *Anomalous dynamical phase in quantum spin chains with long-range interactions*, *Phys. Rev. B* **96**, 104436 (2017).

[17] J. C. Halimeh and V. Zauner-Stauber, *Dynamical phase diagram of quantum spin chains with long-range interactions*, *Phys. Rev. B* **96**, 134427 (2017).

[18] M. Heyl, *Dynamical quantum phase transitions: a survey*, *EPL* **125**, 26001 (2019).

[19] S. De Nicola, A. A. Michilidis, and M. Serbyn, *Entanglement View of Dynamical Quantum Phase Transitions*, *Phys. Rev. Lett.* **126**, 040602 (2021).

[20] B. Zunkovic, M. Heyl, M. Knap, and A. Silva, *Dynamical Quantum Phase Transitions in Spin Chains with Long-Range Interactions: Merging Different Concepts of Nonequilibrium Criticality*, *Phys. Rev. Lett.* **120**, 130601 (2018).

[21] J. Lang, B. Frank, and J. C. Halimeh, *Dynamical Quantum Phase Transitions: A Geometric Picture*, *Phys. Rev. Lett.* **121**, 130603 (2018).

[22] R. Puebla, *Finite-component dynamical quantum phase transitions*, *Phys. Rev. B* **102**, 220302(R) (2020).

[23] S. A. Weidinger, M. Heyl, A. Silva and M. Knap, *Dynamical quantum phase transitions in systems with continuous symmetry breaking*, *Phys. Rev. B* **96**, 134313 (2017).

[24] T. Hashizume, I. P. McCulloch, and J. D. Halimeh, *Dynamical phase transitions in the two-dimensional transverse-field Ising model*, *Phys. Rev. Res.* **4**, 013250 (2022).

[25] A. Sehrawat, C. Srivastava, and U. Sen, *Dynamical phase transitions in the fully connected quantum Ising model: Time period and critical time*, *Phys. Rev. B* **104**, 085105 (2021).

[26] B. Žunkovic, A. Silva and M. Fabrizio, *Dynamical phase transitions an Loschmidt echo in the infinite-range XY model*, *Phil. Trans. R. Soc. A* **374**: 20150160 (2015).

[27] A. Lerose, B. Zunkovic, J. Marino, A. Gambassi, and A. Silva, *Impact of nonequilibrium fluctuations on prethermal dynamical phase transitions in long-range interacting spin chains*, *Phys. Rev. B* **99**, 045128 (2019).

[28] M. Heyl, *Dynamical quantum phase transitions: a review*, *Rep. Prog. Phys.* **81**, 054001 (2018)

[29] P. Cejnar, , P. Stránský, M. Macek, and M. Kloc, *Excited-state quantum phase transitions*, *J. Phys. A: Math. Theor.* **54** (2021) 133001.

[30] R. Puebla, A. Relaño, and J. Retamosa, *Excited-state phase transition leading to symmetry-breaking steady states in the Dicke model*, *Phys. Rev. A* **87**, 023819 (2013).

[31] R. Puebla, and A. Relaño, *Non-thermal excited-state quantum phase transitions*, *EPL* **104**, 50007 (2013).

[32] R. Puebla, and A. Relaño, *Irreversible processes without energy dissipation in an isolated Lipkin-Meshkov-Glick model*, *Phys. Rev. E* **92**, 012101 (2015).

[33] L. F. Santos, M. Távora and F. Pérez-Bernal, *Excited-state quantum phase transitions in many-body systems with infinite-range interaction: Localization, dynamics, and bifurcation*, *Phys. Rev. A* **94**, 012113 (2016).

[34] L. F. Santos and F. Pérez-Bernal, *Structure of eigenstates and quench dynamics at an excited-state quantum phase transition*, *Phys. Rev. A* **92**, 050101(R) (2015).

[35] M. Kloc, D. Šimsa, F. Hanák, P. Ruth Kaprálová-Ždánská, P. Stránský, and P. Cejnar, *Quasiclassical approach to quantum quench dynamics in the presence of an excited-state quantum phase transition*, *Phys. Rev. A* **103**, 032213 (2021).

[36] A. L. Corps and A. Relaño, *Constant of Motion Identifying Excited-State Quantum Phases*, *Phys. Rev. Lett.* **127**, 130602 (2021).

[37] S. Sachdev, *Quantum Phase Transitions*, Cambridge University Press (1999).

[38] H. Lipkin, N. Meshkov, and A. Glick, *Validity of many-body approximation methods for a solvable model: (I). Exact solutions and perturbation theory*, *Nucl. Phys.* **62**, 188 (1965).

[39] S. Dusuel and J. Vidal, *Finite-Size Scaling Exponents of the Lipkin-Meshkov-Glick Model*, Phys. Rev. Lett. **93**, 237204 (2004).

[40] W. D. Heiss, F G Scholtz, and H B Geyer, *The large  $N$  behaviour of the Lipkin model and exceptional points*, J. Phys. A: Math. Gen. **38**, 1843 (2005).

[41] F. Leyvraz and W. D. Heiss, *Large- $N$  Scaling Behavior of the Lipkin-Meshkov-Glick Model*, Phys. Rev. Lett. **95**, 050402 (2005).

[42] O. Castaños, R. López-Peña, J. G. Hirsch, and E. López-Moreno, *Classical and quantum phase transitions in the Lipkin-Meshkov-Glick model*, Phys. Rev. B **74**, 104118 (2006).

[43] P. Ribeiro, J. Vidal, and R. Mosseri, *Thermodynamical Limit of the Lipkin-Meshkov-Glick Model*, Phys. Rev. Lett. **99**, 050402 (2007).

[44] P. Ribeiro, J. Vidal, and R. Mosseri, *Exact spectrum of the Lipkin-Meshkov-Glick model in the thermodynamic limit and finite-size corrections*, Phys. Rev. E **78**, 021106 (2008).

[45] A. Relaño, J. M. Arias, J. Dukelsky, J. E. García-Ramos, and P. Pérez-Fernández, *Decoherence as a signature of an excited-state quantum phase transition*, Phys. Rev. A **78**, 060102(R) (2008).

[46] J. E. García-Ramos, P. Pérez-Fernández, and J. M. Arias, *Excited-state quantum phase transitions in a two-fluid Lipkin model*, Phys. Rev. C **95**, 054326 (2017).

[47] R. Puebla, M.-J. Hwang, and M. B. Plenio, *Excited-state quantum phase transition in the Rabi model*, Phys. Rev. A **94**, 023835 (2016).

[48] M.-J. Hwang, R. Puebla, and M. B. Plenio, *Quantum Phase Transition and Universal Dynamics in the Rabi Model*, Phys. Rev. Lett. **115**, 180404 (2015).

[49] C. M. López and A. Relaño, *Entropy, chaos, and excited-state quantum phase transitions in the Dicke model*, Phys. Rev. E **94**, 012140 (2016).

[50] M. A. Bastarrachea-Magnani, S. Lerma-Hernández, J. G. Hirsch, *Comparative quantum and semi-classical analysis of Atom-Field Systems I: density of states and excited-state quantum phase transitions*, Phys. Rev. A **89**, 032101 (2014).

[51] P. Pérez-Fernández, A. Relaño, J. M. Arias, P. Cejnar, J. Dukelsky, and J. E. García-Ramos, *Excited-state phase transition and onset of chaos in quantum optical models*, Phys. Rev. E **83**, 046208 (2011).

[52] P. Pérez-Fernández, P. Cejnar, J. M. Arias, J. Dukelsky, J. E. García-Ramos, and A. Relaño, *Quantum quench influenced by an excited-state phase transition*, Phys. Rev. A **83**, 033802 (2011).

[53] T. Brandes, *Excited-state quantum phase transitions in Dicke superradiance models*, Phys. Rev. E **88**, 032133 (2013).

[54] M. Kloc, P. Stránský, and P. Cejnar, *Quantum quench dynamics in Dicke superradiance models*, Phys. Rev. A **98**, 013836 (2018).

[55] P. Feldmann, C. Klempt, A. Smerzi, L. Santos, and M. Gessner, *Interferometric Order Parameter for Excited-State Quantum Phase Transitions in Bose-Einstein Condensates*, Phys. Rev. Lett. **126**, 230602 (2021).

[56] Q. Wang and F. Pérez-Bernal, *Signatures of excited-state quantum phase transitions in quantum many-body systems: Phase space analysis*, Phys. Rev. E **104**, 034119 (2021).

[57] A. Relaño, J. Dukelsky, P. Pérez-Fernández, and J. M. Arias, *Quantum phase transitions of atom-molecule Bose mixtures in a double-well potential*, Phys. Rev. E **90**, 042139 (2014).

[58] A. L. Corps, R. A. Molina and A. Relaño, *Chaos in a deformed Dicke model*, J. Phys. A: Math. Theor. **55** (2022) 084001.

[59] A. L. Corps and A. Relaño, *Energy cat states induced by a parity-breaking excited-state quantum phase transition*, Phys. Rev. A (In Press).

[60] P. Reimann, *Foundations of statistical mechanics under experimentally realistic conditions*, Phys. Rev. Lett. **101**, 190403 (2008).

[61] A. L. Corps and A. Relaño, *Dynamical and excited-state quantum phase transitions in collective systems*, Companion article, to appear on arXiv.

[62] L. D'Alessio, Y. Kafri, A. Polkovnikov, and M. Rigol, *From Quantum Chaos and Eigenstate Thermalization to Statistical Mechanics and Thermodynamics*, Adv. Phys. **65**, 239 (2016).

[63] Y. Guryanova, S. Popescu, A. J. Short, R. Silva, and P. Skrzypczyk, *Thermodynamics of quantum systems with multiple conserved quantities*, Nat. Comm. **7**, 12049 (2016).

[64] N. Y. Halpern, P. Faist, J. Oppenheim, and A. Winter, *Micro-canonical and resource-theoretic derivations of the thermal state of a quantum system with noncommuting charges*, Nat. Comm. **7**, 12051 (2016).

[65] N. Y. Halpern, M. E. Beverland, and A. Kalev, *Noncommuting conserved charges in quantum many-body thermalization*, Phys. Rev. E **101**, 042117 (2020).

[66] R. Botet, R. Jullien, and P. Pfeuty, *Size scaling for infinitely coordinated systems*, Phys. Rev. Lett. **49**, 478 (1982).